

See discussions, stats, and author profiles for this publication at: <https://www.researchgate.net/publication/317054108>

Phase Noise Induced by a Vibrating Antenna

Article in IEEE Transactions on Microwave Theory and Techniques · May 2017

DOI: 10.1109/TMTT.2017.2699682

CITATIONS

3

READS

676

1 author:



John Ward

Raytheon Company

69 PUBLICATIONS 2,114 CITATIONS

SEE PROFILE

Phase Noise Induced by a Vibrating Antenna

John S. Ward, *Member, IEEE*

Abstract—When an antenna vibrates, it induces phase noise on the signals that it transmits and receives. This noise source is significant for microwave and millimeter-wave systems operating in high-vibration environments that require low phase noise at small frequency offsets. The purpose of this paper is to derive equations to compute phase noise from vibration parameters and to validate the equations with measurements. It is shown that the induced phase noise varies as f_v^{-4} , where f_v is the frequency of vibration. The results are then compared to the phase noise induced on an oscillator by vibration to determine the oscillator g sensitivity such that the oscillator and antenna phase noise contributions are equal. For state-of-the-art low-g-sensitivity oscillators, the phase noise contribution of the antenna can dominate at vibrational frequencies up to several kilohertz. The vibrational phase noise sensitivity of the antenna is also larger than reported vibrational sensitivity of coaxial cables up to at least 1000 Hz vibrational frequencies and bandpass filters up to 300 to 1000 Hz vibrational frequencies depending on the filter quality factor.

Index Terms—antennas, phase noise, vibration.

I. INTRODUCTION

PRIOR research into the effects of vibration on antennas has largely focused on the vibrational deformation of antennas, especially for the case where the antenna is electrically large. It has been shown that vibration-induced antenna deformation changes antenna patterns, including changing the main beam direction (pointing), increasing beam width, changing null depths and locations, and changing sidelobe levels [1][2]. Task groups chartered by the North Atlantic Treaty Organization (NATO) to study the vibration control of antennas highlight the importance of understanding and mitigating the impacts of vibration on antenna performance. Known as Task Group SET-087 and Task Group SET-131, these studies have demonstrated active vibration suppression systems that improve antenna performance [3]-[5].

The negative impacts of antenna vibration include inducing errors into measured direction-of-arrival (DOA) estimates of radio direction-finding systems [6] as well as degrading radar performance including Moving Target Indicators (MTI) and Synthetic Aperture Radar (SAR) [7]-[9]. Antenna vibration has also been investigated in the context of cosite interference.

Manuscript received August 5, 2016; revised January 31, 2017; accepted March 26, 2017. This document does not contain technology or Technical Data controlled under either the U.S. International Traffic in Arms Regulations or the U.S. Export Administration Regulations.

J. S. Ward is with Raytheon Company Space and Airborne Systems, Fort Wayne, IN 46808 (e-mail: John.S.Ward@Raytheon.com).

Typical transmitted communications signals may be 150 dB stronger than weak received signals. Phase noise on the transmit signal can degrade link performance if the transmit and receive signal are closely spaced in frequency [10]. Antenna vibration has also been studied in the context of phased array feeds for radio telescopes [11].

Even without deformation of the antenna itself, the physical displacement of an antenna in space caused by vibration induces phase errors on signals transmitted and received by the antenna. An alternate interpretation of this phase error is that acceleration induces time-varying Doppler shifts on the signals. This effect is similar to the way that vibration induces phase noise on crystal oscillators. The effect of vibration on oscillators can be understood by considering that static acceleration changes the frequency of a crystal oscillator, and that the change in frequency is directly proportional to the acceleration. This leads to the definition of an oscillator's g sensitivity $\vec{\Gamma}$, which is the constant of proportionality between the acceleration and the resulting fractional frequency shift,

$$\frac{\Delta f}{f_o} = \vec{\Gamma} \cdot \vec{a}, \quad (1)$$

where \vec{a} is the acceleration vector, f_o is the frequency without acceleration, and Δf is the frequency shift induced by the acceleration [12]-[14]. The time-varying changes in oscillator frequency with vibrational acceleration induce phase noise on oscillators in much the same way that the vibration of antennas induces phase noise due to time-varying Doppler shifts.

In contrast to prior work that focuses on the vibration-induced deformation of antennas and antenna arrays, this paper investigates phase noise caused by rigid vibrational displacement of an antenna in space. An expression for the phase noise induced by sinusoidal antenna vibration will be derived, and then this result will be extended to random vibration. These equations are needed to evaluate and mitigate the impact of antenna vibration on system phase noise performance. The results will then be compared to oscillator g sensitivity to provide a simple rule-of-thumb to determine which component contributes the most vibration-induced phase noise to the system, the oscillator or the antenna. State-of-the-art radio-frequency oscillators are available with g sensitivities down to as low as a few times 10^{-12} per g, where g is the acceleration of gravity near the earth's surface [15]-[19]. At this level, the phase noise contribution from the vibration of the antenna will be larger than the phase noise contribution from the vibration of the oscillator at frequency offsets up to several kilohertz.

II. SINUSOIDAL VIBRATION

Assume that an oscillator is generating a pure sine tone at

frequency f_o . Further, assume that this oscillator is unaffected by vibration. The oscillator is feeding an antenna, call it antenna A. Antenna A is vibrating about the coordinate system origin at a frequency f_v . A second antenna called antenna B located at \vec{R} is receiving signals from the vibrating antenna (Fig. 1). Antenna B is stationary and not vibrating.

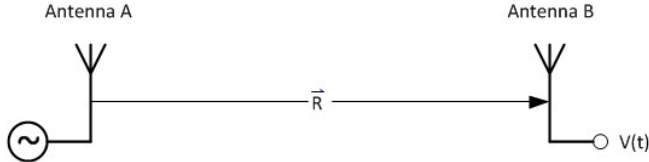


Fig. 1. The vibration of antenna A induces phase noise on the signal received by antenna B.

Antenna A's position as a function of time is given by

$$\vec{x}(t) = \vec{x}_o \sin(2\pi f_v t). \quad (2)$$

In antenna A's reference frame, the phase radiated by antenna A is increasing with time with a constant slope equal to the angular frequency. The phase measured by antenna B is offset by the propagation delay over the distance separating the antennas. Therefore, the phase in radians received by antenna B is

$$\Phi_B(t) = \Phi_A(0) + 2\pi f_o \left[t - \frac{D(t)}{c} \right], \quad (3)$$

where $\Phi_A(0)$ is the initial phase at antenna A, $D(t)$ is the distance separating the two antennas and c is the speed of light in vacuum. The distance separating the antennas is a function of the vibrational displacement in accordance with (2),

$$D(t) = |\vec{R} - \vec{x}_o \sin(2\pi f_v t)|. \quad (4)$$

Define $R \equiv |\vec{R}|$ and $\hat{r} \equiv \vec{R}/|\vec{R}|$. Since for typical systems the antenna separation is on the scale of kilometers and the vibrational displacement is on the scale of millimeters, $R \gg |\vec{x}_o|$ and the first-order approximation of the distance can be used:

$$D(t) = R - (\vec{x}_o \cdot \hat{r}) \sin(2\pi f_v t). \quad (5)$$

Substituting (5) into (3) and choosing the initial phase to be $\Phi_A(0) = \frac{2\pi f_o R}{c}$, the phase of the signal received by antenna B is

$$\Phi_B(t) = 2\pi f_o \left[t + \frac{\vec{x}_o \cdot \hat{r}}{c} \sin(2\pi f_v t) \right]. \quad (6)$$

Since vibration is more often described in terms of acceleration than displacement, it is useful to rewrite (6) in terms of the peak acceleration. The peak acceleration can be found by taking the second derivative of position (2) with respect to time,

$$\vec{a}_p = (2\pi f_v)^2 \vec{x}_o. \quad (7)$$

Note that there are two acceleration peaks of equal magnitude but opposite direction. For convenience, the peak acceleration in the direction of \vec{x}_o was chosen for the definition of \vec{a}_p .

Solve (7) for \vec{x}_o and substitute the result back into (6).

$$\Phi_B(t) = 2\pi f_o t + \frac{1}{2\pi} \frac{\vec{a}_p \cdot \hat{r}}{c} \frac{f_o}{f_v^2} \sin(2\pi f_v t). \quad (8)$$

A. Power Spectrum of the Received Voltage

Ignoring amplitude modulation due to the variation in path loss as the antenna separation changes, the voltage received by antenna B is

$$V(t) = V_R \cos[\Phi_B(t)]. \quad (9)$$

Substituting (8) into (9), the received voltage can be written as

$$V(t) = V_R \cos \left[2\pi f_o t + \frac{1}{2\pi} \frac{\vec{a}_p \cdot \hat{r}}{c} \frac{f_o}{f_v^2} \sin(2\pi f_v t) \right]. \quad (10)$$

Note that the peak acceleration \vec{a}_p is in SI units (m/s^2). For convenience, define β in radians as

$$\beta \equiv \frac{1}{2\pi} \frac{\vec{a}_p \cdot \hat{r}}{c} \frac{f_o}{f_v^2}. \quad (11)$$

Then

$$V(t) = V_R \cos[2\pi f_o t + \beta \sin(2\pi f_v t)]. \quad (12)$$

Expanding (12) to decompose the received voltage as a sum of sinusoidal components,

$$V(t) = V_R \sum_{n=-\infty}^{n=+\infty} J_n(\beta) \cdot \cos[2\pi(f_o + n f_v)t], \quad (13)$$

where J_n is a Bessel function of the first kind [20]. It can be seen from inspection of (13) that the carrier frequency corresponds to $n = 0$ and that the carrier has vibration-induced sidebands at frequency offsets of integer multiples of $\pm f_v$. Fig. 2 shows the fraction of the total received power in the carrier and each of ten frequency offsets for a sinusoidal vibration of 10 Hz with 1 g peak acceleration as a function of carrier frequency. It can be seen that below 10 GHz, the power in the sidebands at $f_o \pm n f_v$ increases by 20n decibels per decade of frequency.

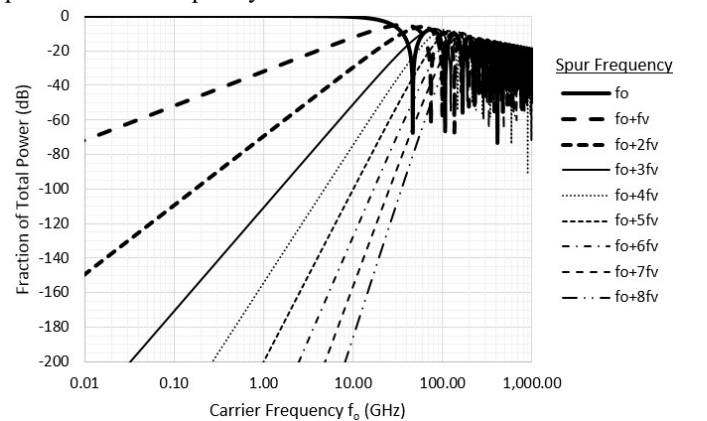


Fig. 2. Fraction of total power in each frequency component for 10 Hz vibration with 1 g peak acceleration.

Fig. 3 shows spectra for several carrier frequencies with 10 Hz sinusoidal vibration and 1 g peak acceleration. At 1 GHz, β equals 0.052 radians, and the spurious signal sidebands fall off strongly with increasing order of the harmonic of the vibration frequency. However, at 100 GHz, β equals 5.2 radians, causing the carrier power to be suppressed

as energy is transferred to a comb at frequency offsets of integer multiples of the vibrational frequency. Ten gigahertz represents the transitional case, with β equal to half a radian.

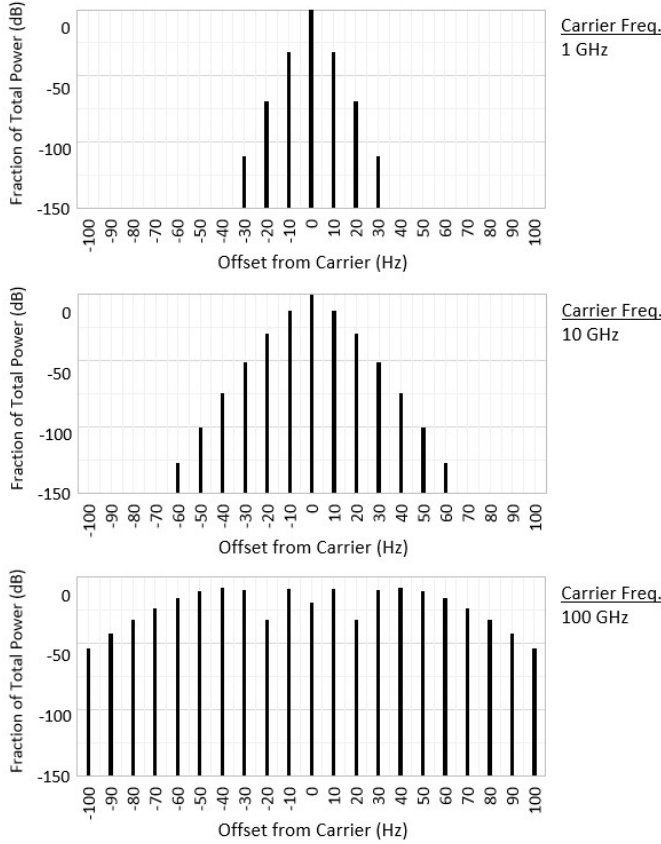


Fig. 3. Spectrum of a carrier with 10 Hz vibration at 1 g peak acceleration.

B. The Weak-Vibration Limit

In most cases, the vibration is sufficiently weak that $|\beta| \ll 1$ radian. Substituting in (11) and rearranging, the weak-vibration limit is equivalent to

$$|\vec{a}_p \cdot \hat{r}| \ll \frac{2\pi c f_v^2}{f_o}. \quad (14)$$

When (14) is valid, it is convenient to approximate the Bessel functions as $J_0(\beta) \approx 1$, $J_1(\beta) \approx \beta/2$ and $J_2(\beta) \approx \beta^2/8$ [20]. Substituting these approximations into (13) gives

$$V(t) \approx V_R \left[\cos(2\pi f_o t) + \frac{\beta}{2} \cos[2\pi(f_o + f_v)t] + \frac{\beta}{2} \cos[2\pi(f_o - f_v)t] + \frac{\beta^2}{8} \cos[2\pi(f_o + 2f_v)t] + \frac{\beta^2}{8} \cos[2\pi(f_o - 2f_v)t] \right] \quad (15)$$

In this limit, (15) shows that the fractional power in each sideband at $f_o \pm f_v$ relative to the power of the carrier at f_o is $\beta^2/4$. In dB, this is¹

$$\frac{P(f_o + f_v)}{P(f_o)} \approx 20 \text{Log}_{10} \left[\frac{1}{4\pi} \frac{\vec{a}_p \cdot \hat{r} f_o}{c f_v^2} \right]. \quad (16)$$

Since (16) is the linear approximation, complex vibrations can be analyzed by decomposing them into a summation of independent sinusoidal components as long as the net phase excursions remain small compared to a radian.

Also in the weak-vibration limit, (15) shows that the power in each sideband at $f_o \pm 2f_v$ is $\beta^4/64$. In dB, this becomes

$$\frac{P(f_o + 2f_v)}{P(f_o)} \approx 40 \text{Log}_{10} \left[\frac{1}{\sqrt{2}} \frac{1}{4\pi} \frac{\vec{a}_p \cdot \hat{r} f_o}{c f_v^2} \right]. \quad (17)$$

III. RANDOM VIBRATION

Random vibrations are typically characterized by their power spectral density (PSD). Call the vibrational PSD in the direction \hat{r} $G(\hat{r}, f_v)$ in units of g^2/Hz , where g is the acceleration of Earth's gravity, i.e., 9.80665 m/s^2 . For a narrow bandwidth Δf_v of random vibration, the vibration is approximately sinusoidal and the peak acceleration can be related to the vibrational PSD.

$$a_p = g \sqrt{2\Delta f_v G(\hat{r}, f_v)}, \quad (18)$$

where the factor of $\sqrt{2}$ scales from RMS to peak values [19]. Using this equation and (8), write the phase received by antenna B in terms of the vibrational PSD, using ϕ_o for the random phase of the vibration at time $t = 0$:

$$\Phi_B(t) = 2\pi f_o t + \frac{1}{2\pi} \frac{g f_o}{c f_v^2} \sqrt{2\Delta f_v G(\hat{r}, f_v)} \sin(2\pi f_v t + \phi_o). \quad (19)$$

Setting the bandwidth Δf_v equal to 1 Hz, the spectral density of vibration-induced phase fluctuations of $\Phi_B(t)$ in radians²/Hz is given by

$$S_\phi(f_v) = \frac{1}{4\pi^2} \frac{g^2 f_o^2}{c^2 f_v^4} G(\hat{r}, f_v). \quad (20)$$

The IEEE definition of phase noise is $\mathcal{L}(f) \equiv \frac{1}{2} S_\phi(f)$ [21]. In units of dB radian²/Hz,

$$\mathcal{L}(f_v) = 10 \text{Log}_{10} \left[\frac{1}{8\pi^2} \frac{g^2 f_o^2}{c^2 f_v^4} G(\hat{r}, f_v) \right]. \quad (21)$$

Fig. 4 shows examples of the effect of random vibration for carrier frequencies ranging from 10 MHz to 100 GHz for random vibration with $0.1 \text{ g}^2/\text{Hz}$ power spectral density. It can be seen that the phase noise increases 20 dB per decade increase in carrier frequency, and falls off 40 dB per decade increase of the vibrational frequency. Phase noise scales as 10 dB per decade of the vibrational PSD.

¹ If referenced to a 1 Hz bandwidth, this is equivalent to the phase noise $\mathcal{L}(f_v)$.

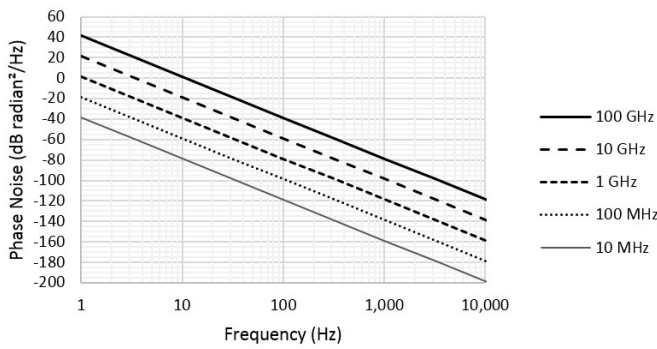


Fig. 4. Phase noise induced by $0.1 \text{ g}^2/\text{Hz}$ random vibration. For small angles, the units are equivalent to dBc/Hz.

IV. EXPERIMENTAL RESULTS

Fig. 5 shows the block diagram of an experimental setup that was used to validate the equations for the phase noise induced by a vibrating antenna. An Agilent E8257D signal generator was connected to a transmit patch antenna. The transmit antenna was vibrated on a shaker table. The transmitted signal was received by a stationary patch antenna and then analyzed with an Agilent E5052B phase noise analyzer.



Fig. 5. Block diagram of the experimental phase noise measurement setup.

Sinusoidal vibrations were measured at a carrier frequency of 9.7 GHz with vibrational frequencies ranging from 15 to 500 Hz and peak accelerations ranging from 0.01 to 1.0 g. Results are shown in Fig. 6 and Fig. 7. The phase noise analyzer uses a phase detector to reject amplitude modulation, such as amplitude modulation caused by the change in path loss with antenna separation. Error bars reflect the specified uncertainty of 4 dB for the phase noise analyzer; the shaker peak acceleration uncertainty is negligible compared to the phase noise analyzer uncertainty. The relative power in each spur was computed by integrating over frequency offset after subtracting the measurement noise floor. The measured data agree with the calculated values within the measurement error.

Random vibrations were measured with a 9.7 GHz carrier with vibration PSD of 0.01, 0.1, and $1.0 \text{ g}^2/\text{Hz}$ over the range 20 to 150 Hz. Results are shown in Fig. 8. The static noise floor was measured with the shaker table turned off, and is dominated by the phase noise of the signal generator and phase noise analyzer. The measurement error caused by the static noise floor was sufficiently small compared to the phase noise analyzer specified uncertainty that it was ignored without subtracting from the measured data. The measured data agree with the calculated values within the measurement uncertainty.

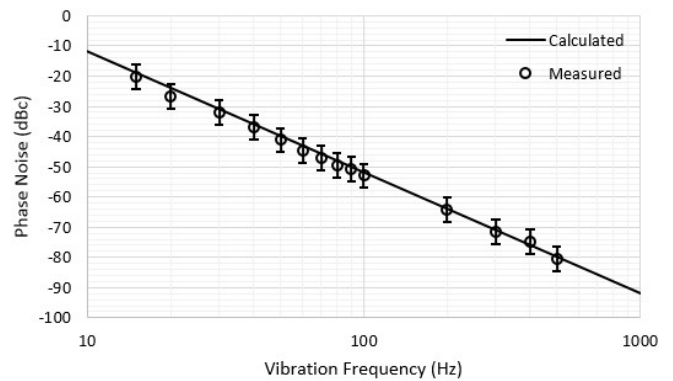


Fig. 6. Measured phase noise spurs on a 9.7 GHz carrier for sinusoidal vibration with 1 g peak acceleration.

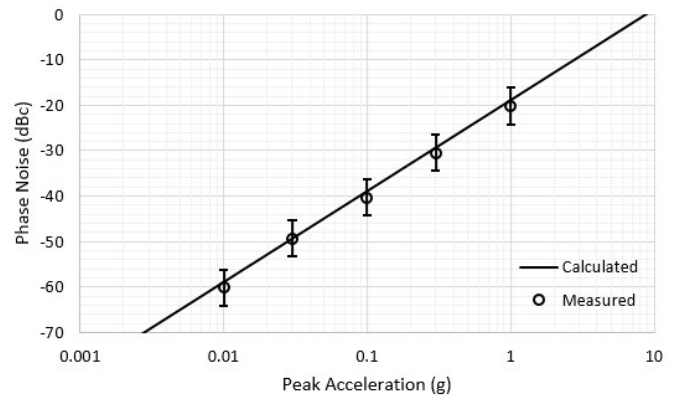


Fig. 7. Measured phase noise spurs on a 9.7 GHz carrier for 15 Hz sinusoidal vibration.

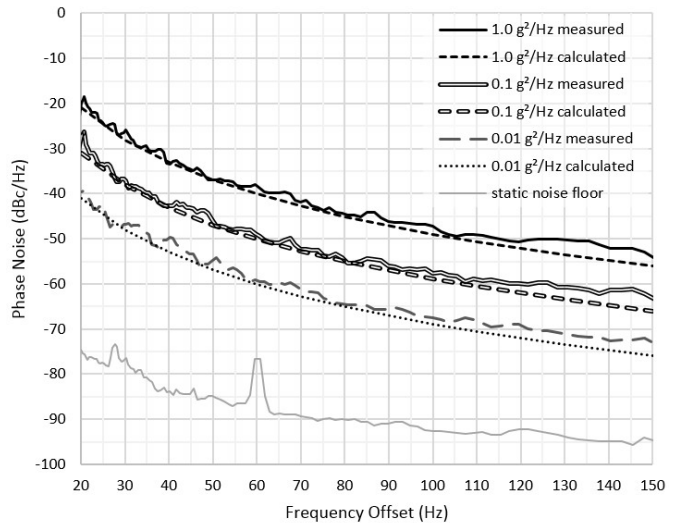


Fig. 8. Measured phase noise of a 9.7 GHz carrier with random vibration from 20 to 150 Hz.

V. COMPARISON TO SENSITIVITY OF OTHER COMPONENTS

A. Oscillator Acceleration Sensitivity

The phase noise induced on an oscillator by vibration can be expressed as

$$\mathcal{L}(f_v) = 20 \text{Log}_{10} \left[\frac{|\bar{\Gamma}| f_o}{f_v} \sqrt{\frac{G(f_v)}{2}} \right], \quad (22)$$

where $\vec{\Gamma}$ is the oscillator acceleration-sensitivity vector defined in (1) in units of $1/g$ and $G(f_v)$ is the acceleration power spectral density in units of g^2/Hz [22]. If the vibrational PSD is isotropic, then (21) and (22) can be equated to find the oscillator g sensitivity where the phase noise contribution of the antenna vibration equals the phase noise contribution of the oscillator vibration. This is true when

$$\Gamma = \frac{g}{2\pi f_v c} \approx \frac{5.2 \cdot 10^{-9}}{f_v}, \quad (23)$$

where f_v is in hertz and Γ is in units of $1/g$. This threshold is independent of the carrier frequency and the vibrational PSD. It can be seen from Fig. 9 that at vibrational frequencies of a few hertz or less, the antenna contribution tends to dominate even for normal oscillators that aren't designed for low g sensitivity. For high-quality low- g -sensitivity oscillators of $\Gamma \approx 10^{-11}$, the antenna vibration dominates up to frequency offsets of several hundred hertz, and when the oscillator is mechanically vibration isolated, which is most effective at frequencies above a few hundred hertz, antenna vibration can dominate at all vibrational frequencies.

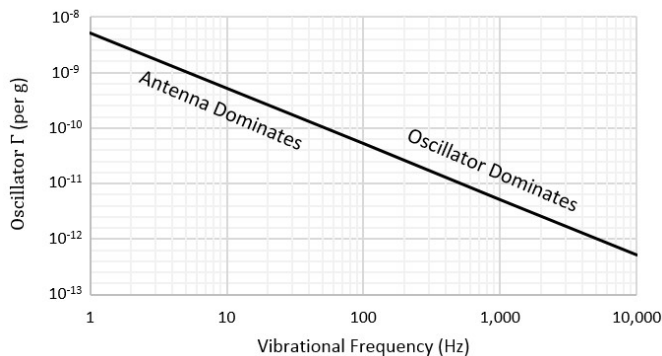


Fig. 9. Threshold where the phase noise contribution from oscillator vibration and antenna vibration are equal.

B. Coaxial Cables

Hati *et al.* measured the phase noise sensitivity of coaxial cables to vibration [23]. Tests were conducted using a 10 GHz carrier with 80 mm lengths of semi-rigid and flexible coaxial cables under $0.001 g^2/Hz$ vibration from 10 Hz to 2000 Hz. These results are compared to the antenna contribution to phase noise in Table I. It is found that the antenna sensitivity is greater than the coaxial cable sensitivity at all measured vibrational frequencies.

TABLE I
PHASE NOISE ON A 10 GHz CARRIER UNDER $0.001 g^2/Hz$ VIBRATION

Offset	Antenna	Flexible Coax	Semi-Rigid Coax
10 Hz	-39 dBc/Hz	-100 dBc/Hz	-112 dBc/Hz
30 Hz	-58 dBc/Hz	-102 dBc/Hz	-140 dBc/Hz
100 Hz	-79 dBc/Hz	-117 dBc/Hz	-130 dBc/Hz
300 Hz	-98 dBc/Hz	-129 dBc/Hz	-130 dBc/Hz
1,000 Hz	-119 dBc/Hz	-125 dBc/Hz	-140 dBc/Hz

C. Filters

Hati *et al.* measured the phase noise sensitivity of 10 GHz bandpass cavity filters to vibration [23]. The effective quality factors of the filters were 3739 and 320. Tests were conducted using a 10 GHz carrier with $0.001 g^2/Hz$ vibration from 10 Hz

to 2000 Hz. It was shown that the high-Q filter was more sensitive to vibration than the low-Q filter. These results are compared to the antenna contribution to phase noise in Table II. It can be seen that the antenna contribution is greater than the filter contribution in all cases except the high-Q filter at 1000 Hz.

TABLE II
PHASE NOISE ON A 10 GHz CARRIER UNDER $0.001 g^2/Hz$ VIBRATION

Offset	Antenna	High-Q filter	Low-Q filter
10 Hz	-39 dBc/Hz	-107 dBc/Hz	-122 dBc/Hz
30 Hz	-58 dBc/Hz	-107 dBc/Hz	-122 dBc/Hz
100 Hz	-79 dBc/Hz	-107 dBc/Hz	-122 dBc/Hz
300 Hz	-98 dBc/Hz	-107 dBc/Hz	-122 dBc/Hz
1,000 Hz	-119 dBc/Hz	-103 dBc/Hz	-122 dBc/Hz

VI. CONCLUSIONS

Phase noise spurs induced by sinusoidal vibration of an antenna have been computed with exact solutions as well as with approximate solutions for weak vibrations. For weak sinusoidal vibrations, the spurs induced by a vibrating antenna scale as the square of the carrier frequency and with the square of the peak acceleration, but fall off with the fourth power of the vibrational frequency. When the vibrational displacement becomes significant compared to the carrier wavelength, nonlinear effects create phase noise spurs offset from the carrier frequency by integer multiples of the vibration frequencies, and vibration can suppress the power at the carrier frequency. Phase noise has also been computed for random vibration PSDs. The phase noise induced by the random vibration of an antenna increases with the square of the carrier frequency, decreases with the fourth power of the vibrational frequency, and increases linearly with the vibrational PSD. For systems based on oscillators with g sensitivity around $\Gamma \approx 10^{-9}$, the phase noise induced by vibration of the antenna dominates over the phase noise induced by vibration of the oscillator for vibration frequencies below a few hertz, independent of carrier frequency and vibration level. For high-quality low- g -sensitivity oscillators around $\Gamma \approx 10^{-11}$, the antenna dominates up to vibrational frequencies of about 500 Hz. For a 10 GHz carrier, the vibration sensitivity of the antenna is larger than reported coaxial cable vibration sensitivities up to 1000 Hz vibrational frequency, and is larger than the vibration sensitivity of cavity filters up to 300 to 1000 hertz depending on the filter Q.

ACKNOWLEDGMENT

The author wishes to thank Garry Ingram and Douglas Engelberth for their contributions to the phase noise measurements.

References

- [1] P. Knott, H. Schippers, D. Medynski, T. Deloues, E. van Lil, J. Verhaever, and F. Gauthier, "Performances of Conformal and Planar Arrays," *Proc. on NATO Symp. on Smart Antennas*, Chester, UK, 2003.
- [2] B. Turetken and M. Celik, "Analysis of Vibration Effects on Surface Matched Cylindrical IFF Array Antenna," *Proc. 7th European Conference on Antennas and Propagation*, Gothenburg, 2013.

- [3] P. Knott, C. Loecker, S. Algermissen, and R. Sekora, "Vibration control and structure integration of antennas and aircraft – Research in NATO-SET-131," *Proc. 7th European Conference on Antennas and Propagation*, Gothenburg, 2013.
- [4] P. Knott, C. Loecker, S. Algermissen, and W. Grüner, "Research on vibration control and structure integration of antennas in NATO/RTTO/SET-131," *Antennas and Propagation Society International Symposium (APSURSI), 2010 IEEE*, 2010.
- [5] H. Schippers, J.H van Tongeren, P. Knott, T. Deloues, P. Lacomme, and M.R. Scherbarth, "Vibrating antennas and compensation techniques - Research in NATO/RTTO/SET 087/RTG 50," *Aerospace Conference, 2007 IEEE*, pp. 1-13, 2007.
- [6] H. Schippers and G. Vos, "On DOA Estimation of Vibrating Antenna Arrays," *2010 IEEE International Symposium on Phased Array Systems and Technology*, pp. 1010-1016, 2010.
- [7] H. Schippers and G. Vos, "Analysis of Vibrating Lightweight Radar Antennas," in *Radar Conference - Surveillance for a Safer World*, 2009.
- [8] E.J. Arnold, J.B. Yan, R.D. Hale, F. Rodriguez-Morales, P. Gogineni, J. Li, and M. Ewing, "Effects of vibration on a wing-mounted ice-sounding antenna array," *IEEE Antennas and Propagation Magazine*, Vol. 56, No. 6, December 2014.
- [9] Y. Qi, Y. Wang, W. Tan, X Yang, P. Huang, and H. Li, "Study on motion compensation of helicopter-borne snapshot imaging radar based on antenna array," *2015 IEEE 5th Asia-Pacific Conf. on Synthetic Aperture Radar (APSAR)*, pp. 58-61, 2015.
- [10] J. M. Wetherington, "Characterization of Passive Spectral Regrowth in Radio Frequency Systems," Ph.D. dissertation, Dept. Elec. Eng., N. C. State Univ., North Carolina, 2013.
- [11] Y. Wu, K. Warnick, and C. Jin, "Design Study of an L-Band Phased Array Feed for Wide-Field Surveys and Vibration Compensation on FAST," *IEEE Trans. on Antennas and Prop.*, vol. 61, no. 6, pp. 3026-3033, June 2013.
- [12] A.W. Warner and W.L. Smith, "Quartz crystal units and precision oscillators for operation in severe mechanical environments," *14th Annual Symp. on Freq. Control*, pp. 200-216, 1960.
- [13] M. Valdois, J. Besson, and J. J. Gagnepain, "Influence of environmental conditions on a quartz resonator," *28th Annual Symp. Freq. Control*, pp. 19-32, 1974.
- [14] R. L. Filler, "The effect of vibration on frequency standards and clocks," *35th Annual Symp. Freq. Control*, pp. 31-39, 1981.
- [15] M. M. Driscoll, "Reduction of quartz oscillator flicker-of-frequency and white phase noise (floor) levels of acceleration sensitivity via use of multiple resonators," *IEEE Trans. Ultrason., Ferroelect., Freq. Control*, vol. 40, no. 4, pp. 427-430, July 1993.
- [16] J. A. Kosinski, "Theory and design of crystal oscillators immune to acceleration: Present state of the art," in *Proc. IEEE/EIA Freq. Control Symp. and Exhibit.*, pp. 260-268, 2000.
- [17] M. Block, O. Mancini, and C. Stone, "Method for achieving highly reproducible acceleration insensitive quartz crystal oscillators," U.S. Patent 20050242893.
- [18] H. Fruehauf, "G-Compensated, Miniature, High Performance Quartz Crystal Oscillators," Frequency Electronics, Inc., Mitchel Field, NY, 2007.
- [19] A. Hati, C. Nelson, and D. Howe, "Vibration-induced PM noise in oscillators and its suppression," National Institute of Standards and Technology, 2009.
- [20] G. N. Watson, *A Treatise on the Theory of Bessel Functions*, 2nd edition, Cambridge University Press, 1966.
- [21] IEEE Standard 1139-2008, "IEEE Standard Definitions of Physical Quantities for Fundamental Frequency and Time Metrology—Random Instabilities," February 27, 2009.
- [22] R. L. Filler, "The Acceleration Sensitivity of Quartz Crystal Oscillators: A Review," *IEEE Trans. on Ultrasonics, Ferroelectrics, and Frequency Control*, Vol. 35, No. 3, May 1988.
- [23] A. Hati, C. W. Nelson, and D. A. Howe, "Vibration-Induced PM and AM Noise in Microwave Components," *IEEE Trans. on Ultrasonics, Ferroelectrics, and Frequency Control*, Vol. 56, No. 10, October 2009.



John S. Ward (M'08) was born in Monticello, Indiana in 1971. He received the Ph.D. degree in physics from the California Institute of Technology, Pasadena, California in 2002. His doctoral research included the development of a 600–700-GHz superconductor–insulator–superconductor (SIS) receiver that he

used to study molecular gas in astronomical sources, as well as the development of software tools for designing and optimizing submillimeter-wave heterodyne receivers.

From 2002 to 2009, Dr. Ward was a Senior Member of the Engineering Staff with the Jet Propulsion Laboratory (JPL), Pasadena, CA, where he led a team that developed local oscillators up to 1.9 THz for the heterodyne instrument on the Herschel Space Observatory. Since 2009, he is a Senior Principal Systems Engineer with the Raytheon Company in Fort Wayne, Indiana.